

Supplementary Notes

In a previous study in which we examined the genome-wide response of *Arabidopsis* to the xenobiotic compound trinitrotoluene (TNT) via cDNA microarrays, we found that *Atwbc19* (At3g55130) was among upregulated genes¹. Given the role of ABC transporters in cellular detoxification we sought to further characterize this gene. Initial characterization of mutants revealed that root growth of *Atwbc19* knockout mutants on media containing kanamycin was much slower than that of other ABC mutants. We specifically compared the kanamycin resistance level of mutants of *Atwbc19* (SALK_107731) and two close homologues *Atwbc18* (SALK_100187) and *Atwbc16* (SALK_119868) that share over 76% similarity in amino acid sequence with *Atwbc19* (see **Supplementary Fig. 5**).

The mutants were T-DNA insertional mutants transformed with plasmid pROK2² containing an *nptII* gene, under the control of the nopaline synthase (*nos*) promoter. Therefore, we also compared their NPTII protein synthesis levels by ELISA assays. On media without kanamycin, there was no significant difference in root growth between the 3 lines. On media with kanamycin, root growth of line SALK_107731 was not different than that of SALK_119868 (0.31 ± 0.04 and 0.30 ± 0.03 cm, respectively) and clearly less than that of SALK_100187 (1.82 ± 0.25 cm) as illustrated in **Supplementary Figure 1**. However, the amount of NPTII protein synthesized was more than 1000-fold higher in the SALK_107731 mutant compared to the other two mutants. Thus, these results strongly suggested that *Atwbc19* had a role in kanamycin resistance while its two close homologues did not. The estimated level of resistance conferred by *Atwbc19*, under the control of its native promoter is equivalent to 1 μ g NPTII per mg fresh weight, an

expression level conferred by the *nos* promoter. It also implied that *Atwbc19* could be used as a kanamycin selection marker to generate plants without the *nptII* gene. The interest in using *Atwbc19* as a selection marker was two-fold. First, the transgenic plants would be valuable to confirm the role of *Atwbc19* without the confounding effect of the *nptII* gene. Second, is the novelty and usefulness of *Atwbc19* as an antibiotic selectable marker.

To examine the subcellular localization of AtWBC19, ten independent transgenic tobacco plants containing an *Atwbc19*-N-terminal *gfp* fusion construct were generated (**Supplementary Fig. 4**). Epifluorescence microscopy revealed that GFP fluorescence in T₀ and T₁ plants could not be detected in aerial part of plants, but could be visualized in root tips (**Supplementary Fig. 4 a,b**). GFP seemed to be directed to vacuoles and was definitely excluded from the nucleus (**Supplementary Fig. 4c**). Because GFP is rapidly degraded in vacuoles under light, it is typically difficult to detect in aerial organs of higher plants³, thus its accumulation in roots in intact plants. The cleavage of an additional peptide at the N or C terminus of GFP is even faster, presumably because unlike the core of GFP it would be more susceptible to attack by proteinases³. This degradation is limited in dark incubated protoplasts. When prepared protoplasts from leaf mesophyll tissue were examined by confocal microscopy, GFP could be visualized in the vacuolar lumen (**Supplementary Fig. 4 d,e,f**). These results suggest that GFP was cleaved from the fusion protein after it reached its target site, the vacuolar membrane, although a mislocalization of the fusion or its degradation products cannot be ruled out.

To gauge the usefulness of *Atwbc19* in a crop species, we initiated *Brassica napus* (canola) transformation with pABC. While preliminary results show fewer putative transgenic calli with pABC compared with pNPT using GUS staining, the 20.3% efficiency (**Supplementary Table 2**) is promising. There is often considerable variability among transformation experiments, small sample sizes were used and kanamycin concentration for canola needs optimization for selection using ABC.

METHODS

Characterization of insertional mutants. Sequence-tagged insertional mutant lines for the three ABC transporters, *Atwbc19* (SALK_107731), *Atwbc18* (SALK_100187) and *Atwbc16* (SALK_119868) were obtained from ABRC *Arabidopsis* knock-out library. Homozygosity was tested by PCR of genomic DNA using 3 primers. Two of the primers are specific to the native gene (5'GACGAACTCGGAAGCGAACA3' and 5'GGTGCAGAGCAGAAGCCAAA3' for *Atwbc19*; 5'GGTCCTGTTCTCAAGCATGTGG3' and 5'AAGAAGCCATCGCTGCAAGTG3' for *Atwbc18*; 5'AAAGCGATTCATAGGTGCTTTTTG3' and 5'CTACACTTGCGCCGATGCTCT3' for *Atwbc16*. The third primer is specific to the T-DNA (5'GCGTGGACCGCTTGCTGCAACT3'). Where the T-DNA is inserted between the two gene specific primers, a smaller fragment is generated allowing the identification of insertion in the gene of interest. The fragment was sequenced to ensure its identification. Kanamycin resistance was assessed by growing the mutants on MSO media with and without 100 mg/l kanamycin. Stratified seeds were germinated on 4 Petri dishes with 6 plants for each line and Petri dishes were placed vertically in a growth

chamber at 25 degrees. Root length was measured after 2 weeks. To quantify NPTII protein levels, total protein was extracted from 100 mg of root and shoot tissue from seedlings germinated on MSO media for 2 weeks, with 2 replicate samples per line. An ELISA was performed using a kit according to the manufacturer's instructions (Agdia, Elkhart, IN, USA).

Subcellular localization. Construction of an N-terminal GFP fusion with *Atwbc19* was performed by amplifying *mgfp5-ER* using forward primer 5'TGCAGGTACCATGAGTAAAGGAGAAGAAGCTTTTC 3' and reverse primer 5' GCTAGGTACCTTTGTATAGTTCATCCATGCC 3'. The amplified fragment no longer had the signal sequence and the ER retention signal. A start codon and *KpnI* sites were introduced on either end that allowed in frame cloning into the *KpnI* site of pNPT-ABC resulting in pNPT-GFP-ABC (**Supplementary Fig. 4**). Roots and leaves from transgenic plants were examined under an epifluorescence microscope (Olympus BX51, Olympus, Melville, New York, USA) or a confocal laser scanning microscope (Leica TCS-SP2, Leica, Heidelberg GmbH, Germany). For confocal microscopy, GFP was excited at 488 nm using an argon laser, and fluorescence emission was recorded in the green channel (500 to 560 nm). To differentiate the GFP signal from chlorophyll autofluorescence in leaf mesophyll protoplasts, fluorescence was also recorded in the red channel (650-720 nm). In the merged image, a GFP specific signal appears green and background fluorescence appears as yellow.

***Brassica napus* transformation.** Hypocotyl segments of *Brassica napus* cv Westar were subjected to *Agrobacterium tumefaciens*-mediated transformation using published methods⁴. A total of at least 70 hypocotyl segments were coincubated with *Agrobacterium* harboring one of two plasmids: pNTP or pABC. Another 70 hypocotyls were coincubated with *Agrobacterium* containing no binary plasmid as a control. After three weeks, hypocotyl segments and calli were subject to GUS staining, and clearly-delimited GUS-positive calli were tallied.

Supplementary References

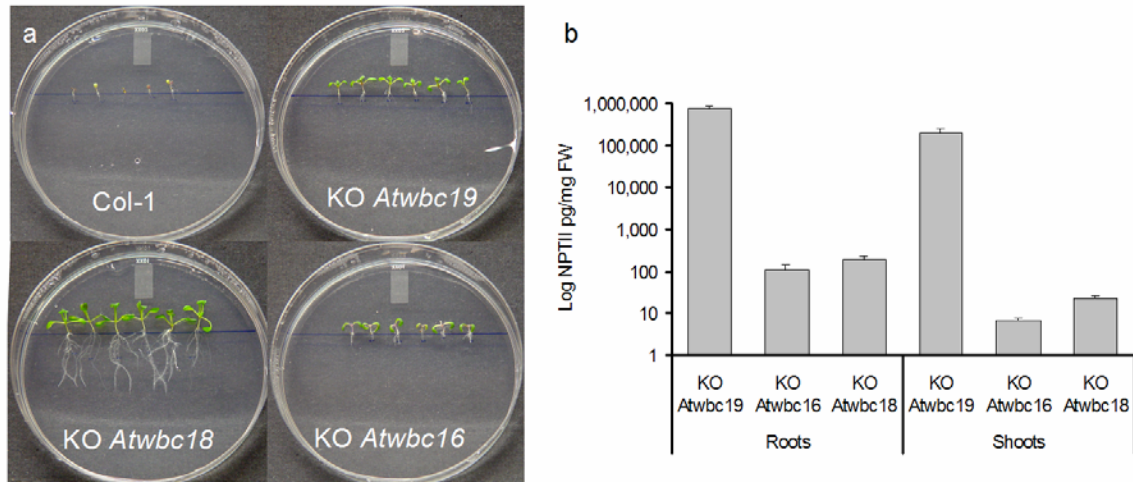
1. Mentewab, A., Cardoza, V., & Stewart, J. Genomic analysis of the response of *Arabidopsis thaliana* to trinitrotoluene as revealed by cDNA microarrays. *Plant Sci.* **168**, 1409-1424 (2005).
2. Baulcombe, D.C., Saunders, G.R., Bevan, M.W., Mayo, M.A., & Harrison, B.D. Expression of biologically-active viral satellite RNA from the nuclear genome of transformed plants. *Nature* **321**, 446-449 (1986).
3. Tamura, K., Shimada, T., Ono, E., Tanaka, Y., Nagatani, A., Higashi, S., Watanabe, M., Nishimura, M., & Hara-Nishimura, I. Why green fluorescent fusion proteins have not been observed in the vacuoles of higher plants. *Plant J.* **35**, 545-555 (2003).
4. Cardoza, V. & Stewart C. N. Jr. Increased *Agrobacterium*-mediated transformation and rooting efficiencies in canola (*Brassica napus* L.) from hypocotyl segment explants. *Plant Cell Rep.* **21**, 599-604. (2003).

Supplementary Table 1 Phenotypic data of 9-week-old greenhouse-grown T₁ tobacco plants. Seeds were surface sterilized and germinated on MS media with 200 mg/l kanamycin for pABC transgenic events and without kanamycin for non transgenic controls. After three weeks, healthy plants were hardened off and transplanted in 8.8 cm pots and grown in a greenhouse. Means and standard deviations are shown. No statistical differences were found at $P=0.05$.

Trait	Non-transgenic control plants	ABC Event 26	ABC Event 28
Number of mature leaves	10.4±1.1	9.2±1.3	9.0±1.3
Plant height (cm)	22.1±3.4	19.8±2.8	20.5±4.4

Supplementary Table 2 Transformation of canola (*Brassica napus*) cv. Westar hypocotyl segments with plasmids pNPT and pABC. The numbers of GUS positive calli were counted 3 weeks after *Agrobacterium*-mediated transformation and transfer to selection media with 100 mg/l kanamycin.

	Number of hypocotyls	Number of GUS positive calli	Percentage per explant
pNPT	70	24	34.3 %
pABC	74	15	20.3 %
No plasmid	75	0	0 %



Supplementary Figure 1 Root growth and NPTII synthesis levels in control

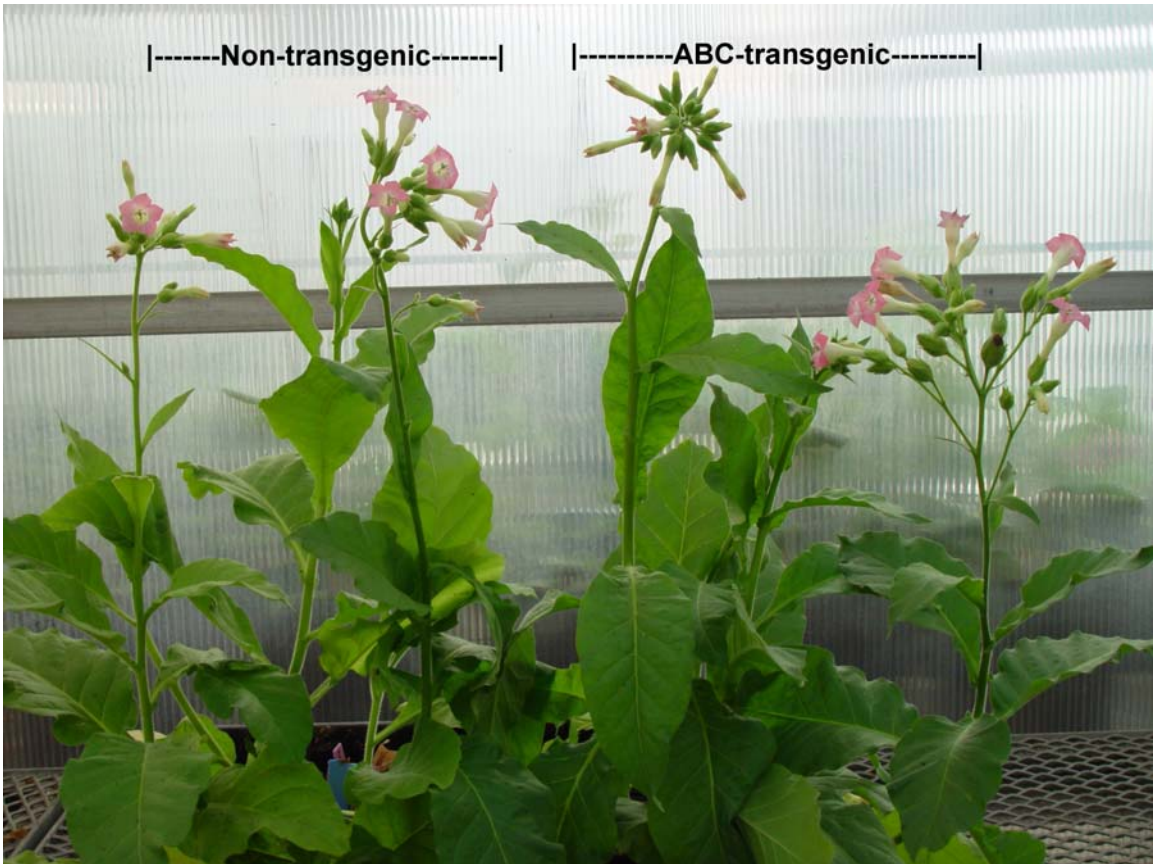
Arabidopsis thaliana Col1 and homozygous insertional knockout mutants (KO) *Atwbc19*

(SALK_107731), *Atwbc16* (SALK_119868) and *Atwbc18* (SALK_100187). Panel a:

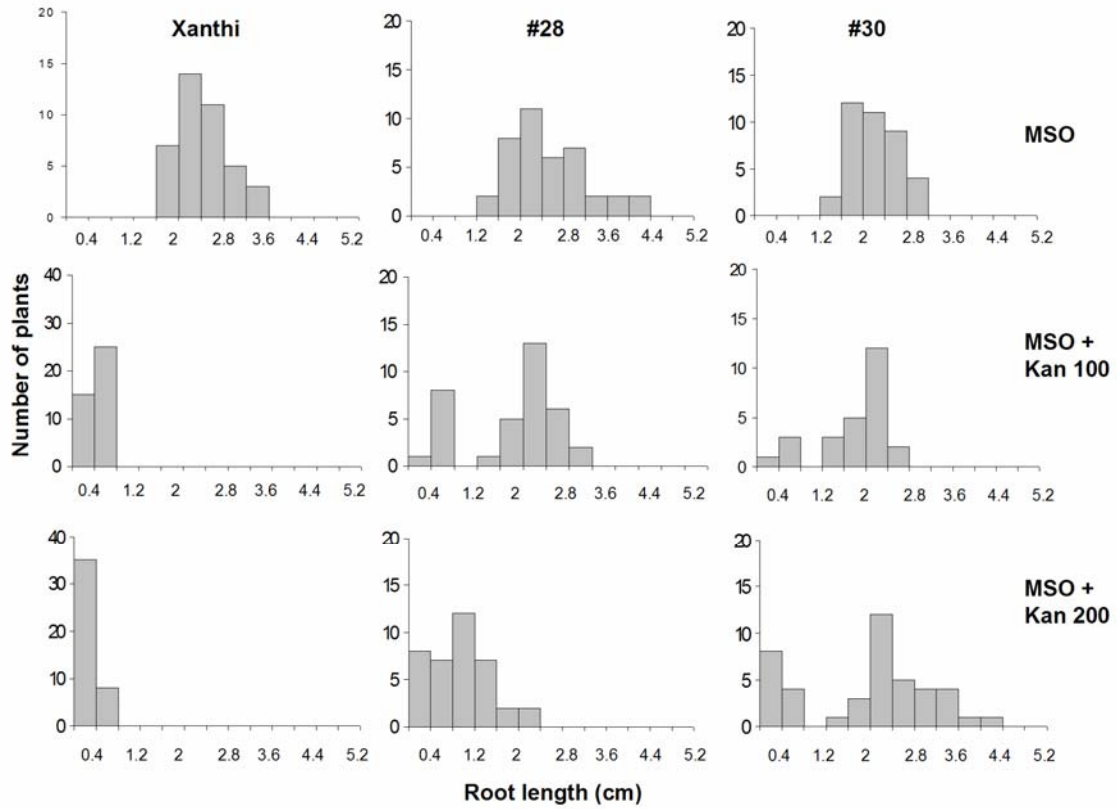
Root growth on vertical MS media containing 100 mg/l kanamycin, 2 weeks after

germination. Panel b: NPTII synthesis levels as measured by ELISA assays in roots and

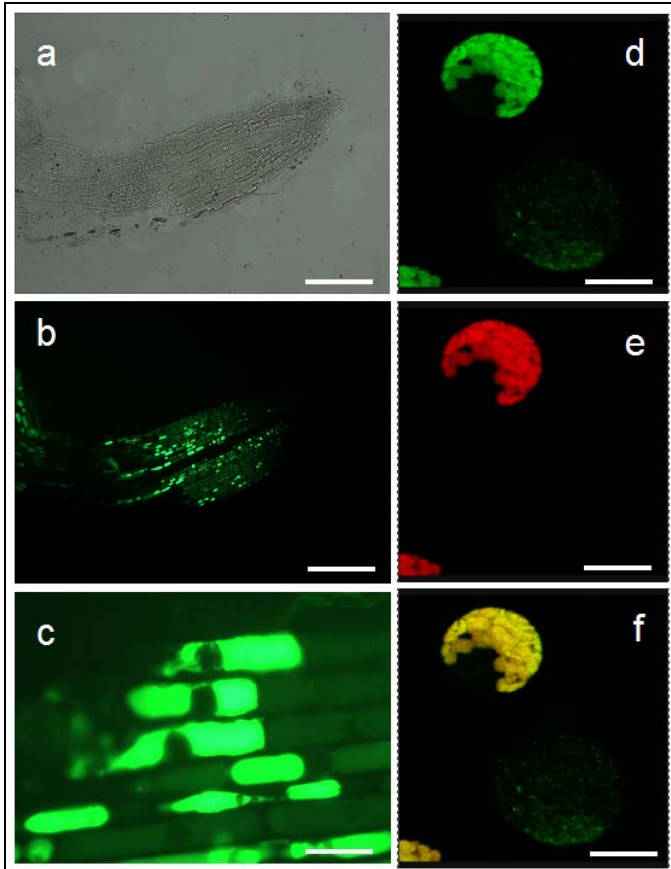
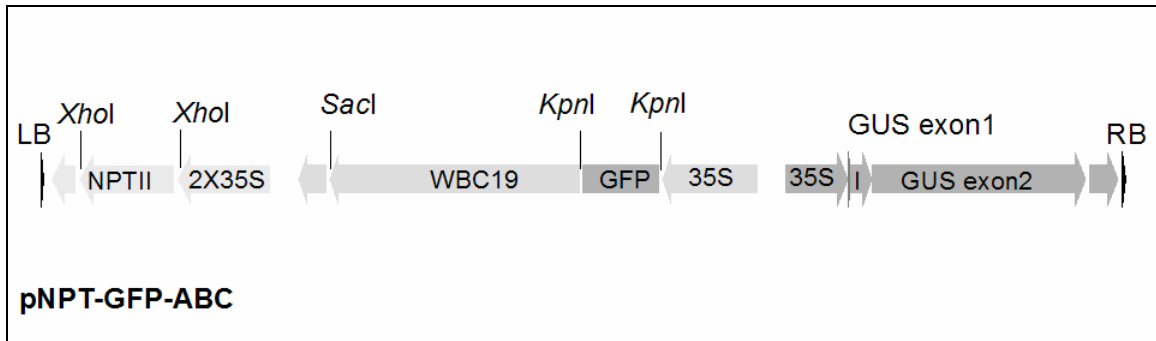
shoots. Bars indicate standard deviations.



Supplementary Figure 2 Twelve-week old non-transgenic and T₁ ABC-transgenic tobacco plants in the greenhouse.



Supplementary Figure 3 Root length distribution frequency of non-transgenic tobacco (Xanthi), and T₁ transgenic lines 28 and 30 grown on MSO media with or without 100 or 200 mg/l kanamycin.



Supplementary Figure 4 Top Panel: T-DNA region of construct used for subcellular localization of AtWBC19. pNPT-GFP-ABC was generated by introducing an N terminal GFP in frame with AtWBC19 at the *KpnI* site of plasmid pNPT-ABC. RB: right border, LB: left border, I: castor bean catalase intron. Bottom panel: Subcellular localization of *Atwbc19*: Fluorescence detection from an N-terminal GFP fusion protein. White light (a) and epifluorescence (b) microscope detection of GFP in root tip cells. Bar = 2 mm. c: epifluorescence detection of GFP in vacuoles. Note that fluorescence is excluded from the nucleus. Bar = 30 μ m. d,e,f: Confocal laser scanning microscope detection of GFP fluorescence in protoplast and vacuole in the green, red and merged channels. GFP is apparently localized in the vacuolar lumen and is excluded from nuclei. Bar = 20 μ m.

